

FRUSTRATED QUANTUM ANTIFERROMAGNETS: APPLICATION OF HIGH-ORDER COUPLED CLUSTER METHOD

J. Richter*, R. Darradi*, R. Zinke*

**Institut für Theoretische Physik, Otto-von-Guericke Universität Magdeburg,
P.O.B. 4120, 39016 Magdeburg, Germany
www.uni-magdeburg.de/itp*

R.F. Bishop⁺

*⁺School of Physics and Astronomy, The University of Manchester,
Sackville Street Building, P.O. Box 88, Manchester, M60 1QD, United Kingdom
www.physics.man.ac.uk*

We report on recent results for strongly frustrated quantum J_1 - J_2 antiferromagnets in dimensionality $d = 1, 2, 3$ obtained by the coupled cluster method (CCM). We demonstrate that the CCM in high orders of approximation allows us to investigate quantum phase transitions driven by frustration and to discuss novel quantum ground states. In detail we consider the ground-state properties of (i) the Heisenberg spin-1/2 antiferromagnet on the cubic lattice in $d = 1, 2, 3$, and use the results for the energy, the sublattice magnetization and the spin stiffness as a benchmark test for the precision of the method; (ii) coupled frustrated spin chains (the quasi-one-dimensional J_1 - J_2 model) and discuss the influence of the quantum fluctuations and the interchain coupling on the incommensurate spiral state present in the classical model; (iii) the Shastry-Sutherland antiferromagnet on the square lattice; and (iv) a stacked frustrated square-lattice Heisenberg antiferromagnet (the quasi-two-dimensional J_1 - J_2 model), and discuss the influence of the interlayer coupling on the quantum paramagnetic ground-state phase that is present for the strictly two-dimensional model.

Keywords: frustration, quantum antiferromagnets, quantum phase transitions, coupled cluster method

1. Introduction

Strongly frustrated quantum magnets have attracted much attention in recent years, both theoretically and experimentally.¹⁻³ In particular, quantum phase transitions have very much become the focus of interest (and see, e.g., Refs. [4-6]). At zero temperature, $T = 0$, there are no thermal fluctuations present and the transitions between ground-state (GS) phases are driven purely by the interplay of quantum-mechanical fluctuations and competition between interactions (e.g., frustration). In particular, novel quantum GS phases, such as valence-bond or spin-liquid phases may appear^{6,7} which do not possess semiclassical magnetic long-range order (LRO).

A basic model which shows strong quantum fluctuations is the spin-1/2 pure Heisenberg antiferromagnet (HAFM). The GS ordering of this quantum HAFM strongly depends on the dimensionality.³ For example, unlike its three-dimensional (3d) and two-dimensional (2d) model counterparts on the cubic or square lattice, respectively, the one-dimensional (1d) pure HAFM (i.e., with nearest-neighbor antiferromagnetic bonds only, and all of equal strength) does not have a Néel-ordered GS.^{6,8} Although the tendency to order is more pronounced in 3d quantum spin systems than in lower-dimensional ones, a magnetically disordered phase can also be observed for 2d and 3d HAFM's when strong frustration is present, e.g., for the J_1 - J_2 model on the square lattice (see, e.g., Refs. [9–21] and references contained therein); or the 2d Shastry-Sutherland antiferromagnet,^{6,22–33} or, in three dimensions, for the HAFM on the pyrochlore lattice^{34,35} or on the stacked kagomé lattice.³⁶

Besides the general interest in frustrated quantum antiferromagnets as rich examples of quantum many-body systems, there is a strong motivation for their theoretical study which is driven by the many recent experiments on quasi-low-dimensional materials that are well described by a frustrated spin-1/2 Heisenberg model. Among many others we mention here (i) the quasi-1d edge-sharing copper oxides like LiCuVO_4 , LiCu_2VO_2 and NaCu_2O_2 ,^{37–40} which were identified as frustrated (with ferromagnetic nearest-neighbor (NN) and antiferromagnetic next-nearest-neighbor (NNN) interactions) quantum helimagnets with an incommensurate spiral GS; (ii) the quasi-2d $\text{SrCu}_2(\text{BO}_3)_2$,^{41,42} which is well described by the Shastry-Sutherland antiferromagnet, and which exhibits a gapped quantum paramagnetic GS; and (iii) the quasi-2d $\text{Li}_2\text{VOSiO}_4$ ^{43,44} which can be described by the J_1 - J_2 model on the square lattice.

The theoretical treatment of the frustrated quantum antiferromagnets is far from being trivial. Though, surprisingly, one can find exact GS's of a simple product nature in some exceptional cases,^{22,45,46} many of the standard many-body methods, such as quantum Monte Carlo techniques, may fail or become computationally infeasible to implement if frustration is present. Other methods, such as density-matrix renormalization group (DMRG) or exact diagonalization techniques, are essentially restricted to low-dimensional systems, at least for the present. Hence, there is considerable interest in any method that can deal with frustrated spin systems in any number of dimensions, including magnetic systems with incommensurate spiral GS's. A method fulfilling this requirement is the coupled cluster method (CCM). This approach, introduced many years ago by Coester and Kümmel,⁴⁷ is one of the most universal and most powerful methods of quantum many-body theory (and for a review of which see, e.g., Ref. [48]). The CCM has previously been applied to various quantum spin systems with much success.^{14,33,49–62} The application to frustrated spin systems was started in the 1990's,^{14,52} and has been developed in more recent years to the point where it has become a powerful tool in this field by including higher orders of approximations in a well-defined truncation scheme.^{33,54,56,57,60,62}

In this paper, we review some recent applications of the CCM to the generic

frustrated quantum spin-1/2 Heisenberg model

$$H = \sum_{i,j} J_{ij} \mathbf{s}_i \cdot \mathbf{s}_j, \quad (1)$$

where the \mathbf{s}_i are the spin operators fulfilling $\mathbf{s}_i^2 = 3/4$, and the J_{ij} are the (competing) exchange coupling parameters.

The paper is organized as follows. In Sec. 2 we illustrate the main features of the CCM, paying special attention to the methodological aspects relevant for the application of the CCM to frustrated magnets. In Sec. 3 we report (as a benchmark test) high-order CCM results for standard unfrustrated lattices in $d = 1, 2, 3$ and compare them with other accurate methods. In Sec. 4 we discuss the influence of quantum fluctuations on GS spiral ordering for quasi-1d J_1 - J_2 spin systems, and in Sec. 5 we report on a CCM treatment of the 2d Shastry-Sutherland model. Finally, Sec. 6 contains a discussion of the GS ordering of a stacked frustrated square-lattice HAFM (the quasi-2d J_1 - J_2 model).

2. The Coupled Cluster Method

The CCM formalism is now briefly outlined. For further details the interested reader is referred to Refs. [50,53–55,59–61]. The starting point for the CCM calculation is the choice of a normalized reference or model state $|\Phi\rangle$, together with a set of (mutually commuting) multi-configurational creation operators $\{C_L^+\}$ and the corresponding set of their Hermitian adjoints $\{C_L\}$,

$$\langle\Phi|C_L^+ = 0 = C_L|\Phi\rangle \quad \forall L \neq 0, \quad C_0^+ \equiv 1; \quad [C_L^+, C_J^+] = 0 = [C_L, C_J]. \quad (2)$$

The operators C_L^+ (C_L) are defined over a complete set of many-body configurations denoted by the set of set-indices $\{L\}$. With the set $\{|\Phi\rangle, C_L^+\}$ the CCM parametrizations of the exact ket and bra GS eigenvectors $|\Psi\rangle$ and $\langle\tilde{\Psi}|$ of our many-body system are then given by

$$|\Psi\rangle = e^S|\Phi\rangle, \quad S = \sum_{L \neq 0} a_L C_L^+; \quad \langle\tilde{\Psi}| = \langle\Phi|\tilde{S}e^{-S}, \quad \tilde{S} = 1 + \sum_{L \neq 0} \tilde{a}_L C_L. \quad (3)$$

The CCM correlation operators, S and \tilde{S} , contain the correlation coefficients, a_L and \tilde{a}_L , which have to be calculated. Once known, all GS properties of the many-body system can clearly be found in terms of them. To find the GS correlation coefficients a_L and \tilde{a}_L , we simply require that the GS energy expectation value $\bar{H} = \langle\tilde{\Psi}|H|\Psi\rangle$ is a minimum with respect to the entire set $\{a_L, \tilde{a}_L\}$, which leads to the GS CCM ket-state and bra-state equations

$$\langle\Phi|C_L^- e^{-S} H e^S |\Phi\rangle = 0, \quad \langle\Phi|\tilde{S} e^{-S} [H, C_L^+] e^S |\Phi\rangle = 0 \quad \forall L \neq 0. \quad (4)$$

For frustrated spin systems an appropriate choice for the CCM model state $|\Phi\rangle$ is often a classical spiral spin state, (i.e., pictorially, $|\Phi\rangle = |\uparrow \nearrow \rightarrow \searrow \downarrow \swarrow \dots\rangle$), which is characterized by a pitch angle α . Such states include the Néel state, for which $\alpha = \pi$. In the quantum model the pitch angle may be modified by quantum

fluctuations. Hence, we do not choose the classical result for the pitch angle but, rather, we consider it as a free parameter in the CCM calculation, which is to be determined by minimization of the CCM GS energy.

In order to find an appropriate set of creation operators it is convenient to perform a rotation of the local axes of each of the spins, such that all spins in the reference state align in the negative z -direction. This rotation by an appropriate angle δ_i of the spin on lattice site i is equivalent to the spin-operator transformation

$$s_i^x = \cos \delta_i \hat{s}_i^x + \sin \delta_i \hat{s}_i^z; \quad s_i^y = \hat{s}_i^y; \quad s_i^z = -\sin \delta_i \hat{s}_i^x + \cos \delta_i \hat{s}_i^z. \quad (5)$$

In this new set of local spin coordinates the reference state and the corresponding creation operators C_L^+ are given by

$$|\hat{\Phi}\rangle = |\downarrow\downarrow\downarrow\downarrow\cdots\rangle; \quad C_L^+ = \hat{s}_i^+, \hat{s}_i^+ \hat{s}_j^+, \hat{s}_i^+ \hat{s}_j^+ \hat{s}_k^+, \dots, \quad (6)$$

where the indices i, j, k, \dots denote arbitrary lattice sites. In the new coordinates the initial Heisenberg Hamiltonian of Eq. (1) becomes

$$\begin{aligned} \hat{H} = & \frac{1}{2} \sum_{i,j} J_{ij} \{ [\cos(\alpha_{ij}) + 1] (\hat{s}_i^+ \hat{s}_j^- + \hat{s}_i^- \hat{s}_j^+) + [\cos(\alpha_{ij}) - 1] (\hat{s}_i^+ \hat{s}_j^+ + \hat{s}_i^- \hat{s}_j^-) \\ & + 2 \sin(\alpha_{ij}) [\hat{s}_i^+ \hat{s}_j^z - \hat{s}_i^z \hat{s}_j^+ + \hat{s}_i^- \hat{s}_j^z - \hat{s}_i^z \hat{s}_j^-] + 4 \cos(\alpha_{ij}) \hat{s}_i^z \hat{s}_j^z \}, \end{aligned} \quad (7)$$

where $\alpha_{ij} \equiv \delta_j - \delta_i$ is the angle between the two interacting spins, and $\hat{s}_i^\pm \equiv \hat{s}_i^x \pm i \hat{s}_i^y$. In the case of the Néel model state \hat{H} becomes much simpler, so that, for example, for the case of NN bonds only, we have $\hat{H} = -J \sum_{\langle i,j \rangle} (\hat{s}_i^+ \hat{s}_j^+ + \hat{s}_i^- \hat{s}_j^- + 2 \hat{s}_i^z \hat{s}_j^z)$.

For the ensuing discussion of the GS properties we concentrate on the GS energy E , the order parameter m and the spin stiffness ρ_s . Within the CCM scheme we have $E = \langle \Phi | e^{-S} H e^S | \Phi \rangle$ and $m = -\frac{1}{N} \langle \tilde{\Psi} | \sum_{i=1}^N \hat{s}_i^z | \Psi \rangle$. The spin stiffness ρ_s can be calculated by imposing a twist on the order parameter of a magnetically long-range ordered system along a given direction, i.e.,

$$\frac{E(\theta)}{N} = \frac{E(\theta=0)}{N} + \frac{1}{2} \rho_s \theta^2 + \mathcal{O}(\theta^4), \quad (8)$$

where $E(\theta)$ is the GS energy as a function of the twist angle θ , and N is the number of sites (and where the interested reader is referred to Ref. [61] for further details).

The CCM formalism is exact if we take into account all possible multispin configurations in the correlation operators S and \tilde{S} . However, in general, this is impossible to do in practice for a quantum many-body system. Hence, it is necessary to use approximation schemes in order to truncate the expansions of S and \tilde{S} in Eq. (3) in any practical calculation. A quite general approximation scheme is the so-called SUB n - m approximation. In this approximation all correlations in the correlation operators S and \tilde{S} are taken into account which span a range of no more than m contiguous sites and contain only n or fewer spins. In most cases the SUB n - n scheme is used (i.e., with $n = m$), and it is then (for spin-1/2 systems) called the LSUB n scheme. To find all different fundamental configurations entering S and \tilde{S} at a given level of LSUB n approximation we use lattice symmetries and, where possible, any exact conservation laws.

Since the LSUB n approximation becomes exact in the limit $n \rightarrow \infty$, it is useful to extrapolate the 'raw' LSUB n results to the limit $n \rightarrow \infty$. Although an exact scaling theory for the LSUB n results is not known, there is some empirical experience^{33,53–55,62} indicating how the physical quantities for spin models might scale with n . For the GS energy we employ^{54,55}

$$E(n) = a_0 + a_1 \frac{1}{n^2} + a_2 \left(\frac{1}{n^2} \right)^2. \quad (9)$$

Furthermore, we note that it may be useful to discard the LSUB2 results for the extrapolation, because generally they fit poorly to the asymptotic behavior.⁵⁵ For the order parameter and the stiffness one utilizes^{55,61} an extrapolation law with leading power $1/n$, i.e.,

$$A(n) = b_0 + b_1 \frac{1}{n} + b_2 \left(\frac{1}{n} \right)^2. \quad (10)$$

However, there is some experience that when applied to systems showing an order-disorder quantum phase transition this kind of extrapolation tends to overestimate the parameter region where magnetic LRO exists, i.e. to yield too large critical values for the exchange parameter driving the transition.^{33,54,58,61} The reason for such behavior might derive from the change of the scaling near a critical point. Hence, in addition to the extrapolation rule of Eq. (10) for the order parameter m , we also use a leading 'power-law' extrapolation^{33,55,61} given by

$$m(n) = c_0 + c_1 \left(\frac{1}{n} \right)^{c_2}, \quad (11)$$

where the leading exponent c_2 is determined directly from the LSUB n data.

3. The CCM for the Pure HAFM on Cubic Lattices for $d = 1, 2, 3$

During the last few years the running time and memory requirements of the original CCM code have been considerably improved.^{60,63} Consequently, it is now possible to run higher levels of approximation by using an improved parallelization procedure. In this Section we present a collection of CCM results for the (unfrustrated) pure HAFM (i.e., with the Hamiltonian of Eq. (1) with $J_{ij} = 1$ for NN bonds, and $J_{ij} = 0$ otherwise) on some basic lattices, and compare them with the most accurate results obtained by other methods. While some of the CCM results have already been published elsewhere,^{55,61} we also present here the new unpublished results from higher levels of approximation. The results are shown in Tables 1, 2 and 3, in which the entries shown in boldface are the new ones.

4. The Quasi-One-Dimensional J_1 - J_2 Model

One-dimensional quantum spin systems like the frustrated J_1 - J_2 -model have attracted much attention over many years.⁸ The physics of such quantum spin systems

Table 1. Data for the spin-1/2 linear-chain pure HAFM. N_f is the number of fundamental configurations for the Néel reference state, E/N is the GS energy per spin and m is the sublattice magnetization. The LSUB n results are extrapolated using Eq. (9) for E/N and Eq. (10) (in parentheses, Eq. (11)) for m .

linear chain	N_f	E/N	m
LSUB2	1	-0.41667	0.33333
LSUB4	3	-0.43627	0.24839
LSUB6	9	-0.44002	0.20789
LSUB8	26	-0.44137	0.18297
LSUB10	81	-0.44200	0.16562
LSUB12	267	-0.44234	0.15263
LSUB14	931	-0.44255	0.14240
LSUB16	3362	-0.44269	0.13408
Extrapolated CCM	-	-0.44315	0.07737 (-0.01086)
Bethe ansatz ⁶⁶	-	-0.44315	0.0

Table 2. Data for the spin-1/2 square-lattice pure HAFM. N_f is the number of fundamental configurations for the Néel (in parentheses, for the spiral) reference state, E/N is the GS energy per spin, m is the sublattice magnetization and ρ_s is the spin stiffness. The LSUB n results are extrapolated using Eq. (9) for E/N , Eq. (10), (in parentheses, Eq. (11)) for m and Eq. (10) for ρ_s .

square lattice	N_f	E/N	m	ρ_s
LSUB2	1 (3)	-0.64833	0.42071	0.2574
LSUB4	7 (40)	-0.66366	0.38240	0.2310
LSUB6	75 (828)	-0.66700	0.36364	0.2176
LSUB8	1287 (21124)	-0.66817	0.35242	0.2097
LSUB10	29605 (586787)	-0.66870	0.34483	-
Extrapolated CCM	-	-0.66936	0.31024 (0.28073)	0.1812
3rd order SWT ⁶⁴	-	-0.66931	0.3069	0.1747
QMC ⁶⁷	-	-0.66944	0.3070	0.1852

Table 3. Data for the spin-1/2 simple-cubic lattice pure HAFM. N_f is the number of fundamental configurations for the Néel (in parentheses, for the spiral) reference state, E/N is the GS energy per spin, m is the sublattice magnetization and ρ_s is the spin stiffness. The LSUB n results are extrapolated using Eq. (9) for E/N , Eq. (10), (in parentheses, Eq. (11)) for m and Eq. (10) for ρ_s .

cubic lattice	N_f	E/N	m	ρ_s
LSUB2	1 (4)	-0.89076	0.45024	0.2527
LSUB4	9 (106)	-0.90043	0.43392	0.2416
LSUB6	181 (5706)	-0.90180	0.42860	0.2380
LSUB8	8809 (444095)	-0.90214	0.42626	-
Extrapolated CCM	-	-0.90247	0.42054 (0.42141)	0.2312
3rd order SWT ⁶⁸	-	-0.9025	0.4227	0.2343

is often remarkably different from that of their corresponding classical counterparts, with a rich variety of different quantum GS's. As already mentioned in Sec. 1, novel edge-sharing copper oxides like LiCuVO_4 and NaCu_2O_2 ,³⁷⁻⁴⁰ that were identified as quantum helimagnets with ferromagnetic NN and frustrating antiferromagnetic

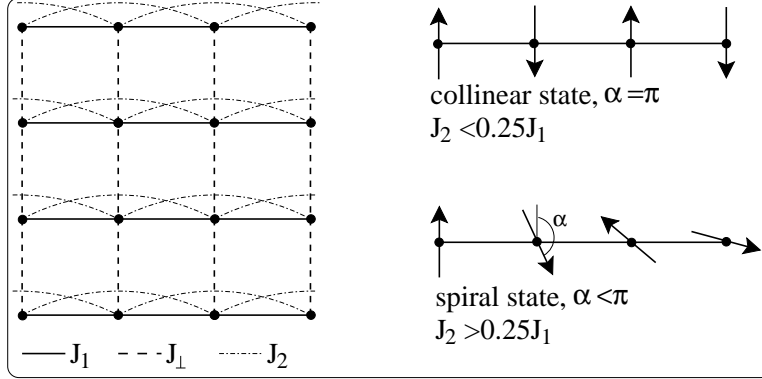


Fig. 1. Illustration of the quasi-1d J_1 - J_2 model and the reference states $|\Phi\rangle$ used for our CCM calculations.

NNN bonds, have stimulated a great deal of renewed interest in frustrated Heisenberg chains. In these materials a finite interchain coupling is also present, which in turn may lead to a low-temperature phase transition to a magnetically ordered phase.

Therefore, we consider in this section the following quasi-1d spin-1/2 J_1 - J_2 Heisenberg model,

$$H = \sum_n \left(J_1 \sum_i \mathbf{s}_{i,n} \cdot \mathbf{s}_{i+1,n} + J_2 \sum_i \mathbf{s}_{i,n} \cdot \mathbf{s}_{i+2,n} \right) + J_\perp \sum_{i,n} \mathbf{s}_{i,n} \cdot \mathbf{s}_{i,n+1}, \quad (12)$$

where n labels the chains, J_\perp is the interchain coupling, J_1 is the in-chain NN coupling and J_2 the in-chain NNN coupling, as shown in Fig. 1. We fix J_1 to $J_1 = 1$ (for the antiferromagnetic case) or to $J_1 = -1$ (for the ferromagnetic case) and consider $J_2 \geq 0$ (which is frustrating in both cases) and $J_\perp \geq 0$. The case $J_\perp = 0$ corresponds to the strictly 1d case.

The classical system is characterized by a second-order transition from a collinear phase to a non-collinear spiral phase at $|\frac{J_2}{J_1}| = 0.25$. For $J_2 \geq |J_1|$ the classical spiral (pitch) angle α_{cl} is given by $\alpha_{cl} = \arccos(-0.25J_1/J_2)$. Note that in the classical model neither the pitch angle α_{cl} nor the transition point $|\frac{J_2}{J_1}| = 0.25$ depends on the interchain coupling J_\perp .

From the experimental point of view it is of interest to discuss the influence of quantum fluctuations on the pitch angle. Furthermore the question arises whether in the quantum model the interlayer coupling J_\perp does or does not influence either or both of the pitch angle and the transition point. While the influence of quantum fluctuations on the pitch angle for $J_\perp = 0$ has been discussed previously in the literature,^{52,69-71} this question has not been considered for finite $J_\perp > 0$ so far. Furthermore, any effect which a finite J_\perp may have on the transition point has also not been considered in the literature. To discuss this point we use the CCM for the model of Eq. (12) at the same level of approximation (viz., SUB2-3) as in Ref. [52].

In that paper it was demonstrated that the SUB2-3 approximation for strictly 1d systems leads to results of comparable accuracy to those obtained using the DMRG method. For the SUB2-3 approximation the relevant CCM equations can be found in closed analytical form, even for nonzero values of J_{\perp} .

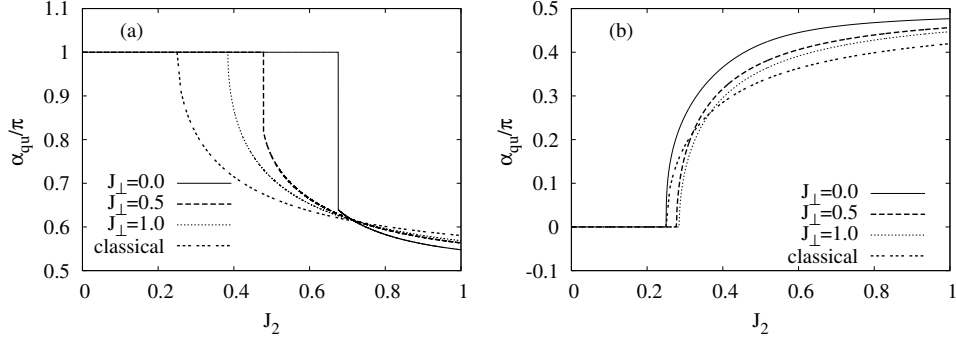


Fig. 2. The quantum pitch angle α_{qu} versus J_2 for the two cases (a) $J_1 = 1$ and (b) $J_1 = -1$ in the CCM SUB2-3 approximation, compared with the classical result.

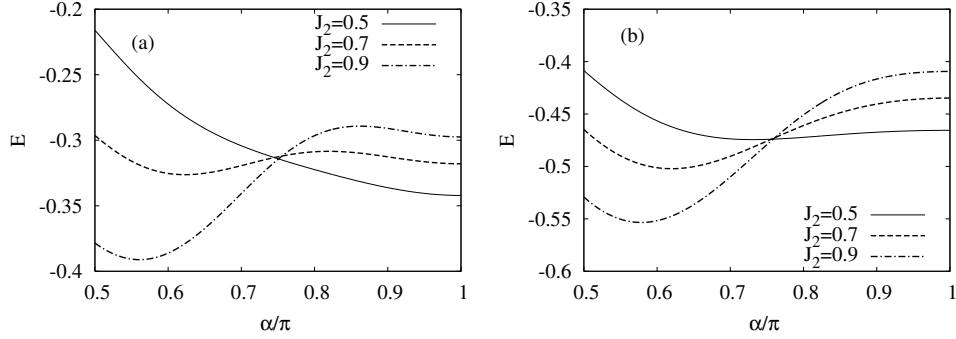


Fig. 3. Ground-state energy per spin in the CCM SUB2-3 approximation as a function of the pitch angle α for different (fixed) values of the NNN frustration strength J_2 and antiferromagnetic NN bonds with $J_1 = 1$, for the two cases (a) $J_{\perp} = 0$ and (b) $J_{\perp} = 0.7J_1$. The quantum pitch angle α_{qu} shown in Fig. 2 corresponds to the absolute minimum of the energy E .

As quantum fluctuations may lead to a ‘quantum’ pitch angle α_{qu} that is different from the classical value α_{cl} , we consider the pitch angle in the reference state as a free parameter. We then determine α_{qu} by minimizing the CCM energy $E(\alpha)$ with respect to α . Some results for the pitch angle α_{qu} of the quantum model are presented in Fig. 2. We have checked explicitly, that for $J_{\perp} = 0$ our results coincide with those of Ref. [52]. (We note that due to the different definitions of the Hamiltonian parameters that agreement is not obvious). For antiferromagnetic J_1

and weak interchain coupling J_{\perp} we find, contrary to the behavior of the classical system, a first-order transition from a collinear phase to a spiral phase, i.e., the quantum pitch angle jumps from $\alpha_{\text{qu}} = \pi$ (in the collinear phase) to $\alpha_{\text{qu}} < \pi$ (in the spiral phase). This is illustrated in Fig. 3 by the energy curves $E(\alpha)$, which show a typical first-order scenario for $J_{\perp} = 0$ compared with a typical second-order scenario for $J_{\perp} = 0.7J_1$. Furthermore, the transition point is both shifted to larger values of $J_2 > 0$ than in the classical case (and cf. Refs. [52,69,70]), and does now depend on J_{\perp} . For increasing J_{\perp} the transition point is shifted towards the classical value (but even for $J_{\perp} = J_1$ it remains significantly above the classical value), and for large enough J_{\perp} the transition between the collinear and the spiral phase becomes continuous.

For ferromagnetic $J_1 = -1$ one has, in complete analogy to the classical system, a second-order transition from the collinear to a spiral phase at $J_2 = 0.25$ when $J_{\perp} = 0$, which is in agreement with earlier considerations.^{56,71} However, for $J_2 > 0.25|J_1|$ the quantum pitch angle deviates from the classical value and depends on the interlayer coupling J_{\perp} . There is also a shift of the transition point for increasing values of J_{\perp} towards larger values of J_2 .

A common feature for both cases (i.e., $J_1 = -1$ and $J_1 = +1$) is, that for increasing values of J_2 the quantum pitch angle approaches its limiting value $\pi/2$ much faster than for the classical model.

The general behavior discussed above can be qualitatively related to the strength of quantum fluctuations (and see, e.g., the discussion in Refs. [33,54,56]), which themselves depend on the values of the exchange parameters of the model. In general, quantum fluctuations tend to stabilize collinear phases. Consequently, for the model with the strongest fluctuations, namely the strictly 1d antiferromagnetic model ($J_{\perp} = 0, J_1 = 1$), the transition to the non-collinear GS takes place for largest J_2 (cf. Fig. 2a). Increasing the interchain coupling then reduces the strength of the quantum fluctuations, which leads to a shift of the transition point to smaller values of J_2 . In the case of the strictly 1d chain with ferromagnetic $J_1 = -1$ and $J_2 < 0.25|J_1|$, the GS is the fully polarized ferromagnetic state, which does not exhibit any quantum fluctuations. As a result the transition point is the same as in the classical model, but the quantum pitch angle starts to deviate from the classical value immediately if $J_2 > 0.25|J_1|$.

Finally, we emphasize that we did not speculate on possible spiral LRO. For strictly 1d systems it is clear that there is no magnetic LRO and the quantum pitch angle discussed above corresponds to incommensurate short-range correlations.

5. A Frustrated Heisenberg Antiferromagnet on the Square Lattice: The Shastry-Sutherland Model

As already mentioned in Sec. 1, the Shastry-Sutherland model, first introduced some 25 years ago,²² has attracted much attention in connection with experiments on $\text{SrCu}_2(\text{BO}_3)_2$. The model is characterized by a special arrangement of frustrating

NNN J_2 bonds on the square lattice, as shown in Fig. 4. Its Hamiltonian reads

$$H = J_1 \sum_{\langle i,j \rangle} \mathbf{s}_i \cdot \mathbf{s}_j + J_2 \sum_{\{i,k\}} \mathbf{s}_i \cdot \mathbf{s}_k, \quad (13)$$

where the sum on $\langle i,j \rangle$ runs over all NN bonds and the sum on $\{i,k\}$ runs only over the selected NNN bonds shown in Fig. 4. In what follows we set $J_1 = 1$ and consider

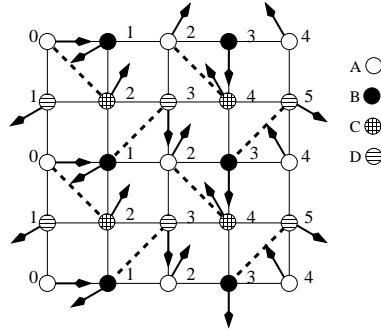


Fig. 4. Illustration of the Shastry-Sutherland model with antiferromagnetic NN bonds $J_1 = 1$ (solid lines) and NNN bonds J_2 (dashed lines), together with its classical spiral state. The spin orientations at lattice sites n are given by the angles $\theta = n\alpha_{cl}$, where $n = 0, 1, 2, \dots$, and α_{cl} is the characteristic pitch angle of the classical spiral state. The state is shown for $\alpha_{cl} = 5\pi/6$ and $n = 0, 1, \dots, 5$.

the case of (frustrating) $J_2 > 0$. Although the GS of this model is well understood in both the limits of small J_2 and large J_2 , the GS phase at intermediate values of J_2 is still a matter of discussion.^{6,23-33} The CCM treatment of this model, briefly reviewed in this Section, is explained in more detail in Ref. [33].

We start with the classical GS of the Shastry-Sutherland model. It is the collinear Néel state for $J_2/J_1 \leq 1$, but a non-collinear spiral state for $J_2/J_1 > 1$ (and see Fig. 4 and Refs. [23,25]), with a characteristic pitch angle α_{cl} given by $\alpha_{cl} = \pi$ for $J_2 \leq J_1$ and $\alpha_{cl} = \pi - \arccos(J_1/J_2)$ for $J_2 > J_1$. The transition from the collinear Néel state to the non-collinear spiral state at $J_2/J_1 = 1$ is of second order for the classical model. We note further that there are only two different angles between interacting spins, namely α_{cl} for the J_1 couplings and $-2\alpha_{cl}$ for the J_2 couplings.

Similarly as we did for the quasi-1d J_1 - J_2 model we now calculate the GS energy as a function of J_2 using as reference state a spiral state as shown in Fig. 4. Again, we find that due to quantum fluctuations the onset of the spiral phase in the quantum model is shifted to higher values of J_2 , and the transition between the collinear and the spiral states becomes discontinuous, as seen from Fig. 5a. We conclude, that the collinear Néel state is the favored CCM reference state up to values $J_2 \approx 1.5J_1$.

It is known from the early paper of Shastry and Sutherland²² that for large J_2 the quantum GS of the model of Eq. (13) is a rotationally-invariant orthogonal-dimer state given by $|\Psi\rangle_{\text{dimer}} = \prod_{\{i,j\}_{J_2}} [|\uparrow_i\rangle|\downarrow_j\rangle - |\downarrow_i\rangle|\uparrow_j\rangle]/\sqrt{2}$, where i and

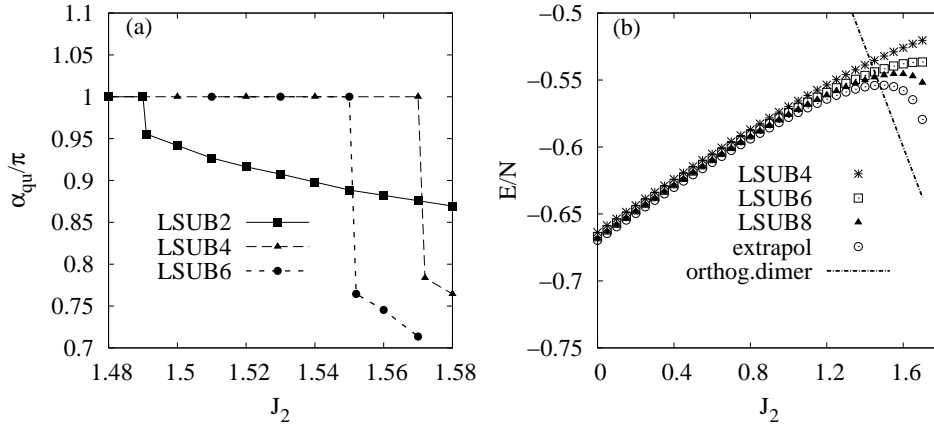


Fig. 5. (a) The quantum pitch angle α_{qu} for the Shastry-Sutherland model with $J_1 = 1$ as a function of J_2 , calculated within the CCM-LSUB n approximation with $n = 2, 4, 6$; and (b) the GS energy per spin as a function of J_2 of (i) the collinear Néel phase obtained within the CCM LSUB n approximation scheme with $n = 4, 6, 8$ and its extrapolated $n \rightarrow \infty$ value using Eq. (9), and (ii) the orthogonal-dimer state.

j correspond to those sites which cover the J_2 bonds. The energy per site of this state is $E_{\text{dimer}}/N = -3J_2/8$. We compare its energy in Fig. 5b with that of the CCM GS obtained with the collinear Néel state as reference state. Our results demonstrate that the orthogonal-dimer state has lower energy than the Néel phase for $J_2 \gtrsim 1.477J_1$, i.e., significantly before the point where the spiral CCM phase has lower energy than the collinear CCM phase. We note that we also checked that $|\Psi\rangle_{\text{dimer}}$ similarly remains the state of lowest energy in the region where the non-collinear spiral phase has lower energy than the Néel phase. We conclude that there is no spiral GS phase in the quantum model. The critical value $J_2^d = 1.477J_1$ where the transition to the orthogonal-dimer phase takes place obtained by the CCM is in good agreement with results obtained by other methods (and see, e.g., Table 2 in Ref. [31]).

So far we have mainly discussed the energy of competing GS phases. The next question we would like to discuss is the question of the stability of the Néel LRO in the frustrated regime. For that purpose we calculate the order parameter (viz., the sublattice magnetization) m within the LSUB n approximation scheme up to $n = 8$ and extrapolate to $n \rightarrow \infty$ using the extrapolation scheme of Eq. (11). The results are shown in Fig. 6a. The extrapolated data clearly demonstrate that the LRO vanishes before the orthogonal-dimer state becomes the GS. The transition from Néel LRO to magnetic disorder is of second order. Hence, in agreement with previous investigations (and see, e.g., Ref. [31]), we come to the second important conclusion that there exists an intermediate magnetically disordered phase. The critical value $J_2^c \approx 1.14J_1$ where the Néel LRO breaks down agrees well with the corresponding value calculated by series expansion techniques as given, for example,

in Table 2 of Ref. [31].

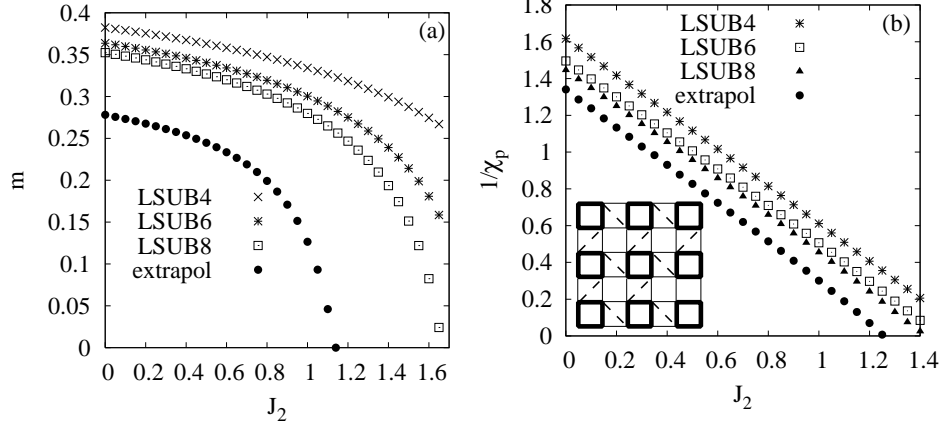


Fig. 6. (a) The sublattice magnetization m versus J_2 obtained within the CCM LSUB n approximation with $n = 4, 6, 8$ and extrapolated to $n \rightarrow \infty$ using Eq. (11); and (b) the inverse susceptibility $1/\chi_p$ versus J_2 obtained within the CCM LSUB n approximation with $n = 4, 6, 8$ and extrapolated to $n \rightarrow \infty$ using Eq. (10). Inset: Pattern of plaquette valence bond order.

The nature of the nonmagnetic GS in the region $1.14J_2 \lesssim J_2 \lesssim 1.477J_2$ is a matter of some controversy in the literature. A favored candidate is a plaquette singlet phase.^{25,26} To address this question we follow similar reasoning to that used in Ref. [21] and consider the response of the spin system to a field F_p given by

$$F_p = \delta \sum_{x,y} [(-1)^x \mathbf{s}_{x,y} \cdot \mathbf{s}_{x+1,y} + (-1)^y \mathbf{s}_{x,y} \cdot \mathbf{s}_{x,y+1}], \quad (14)$$

where x, y are components (integer numbers) of the lattice vectors of the square lattice. This field corresponds to a plaquette valence bond order (as illustrated in the inset of Fig. 6b), which breaks the lattice symmetry. Thus, we use the CCM with the Néel state as reference state to calculate the energy per site $e(J_1, J_2, \delta)$ for $H + F_p$, namely the Hamiltonian of Eq. (13) perturbed by the additional term of Eq. (14). The susceptibility χ_p is then defined as²¹

$$\chi_p = - \left. \frac{\partial^2 e}{\partial \delta^2} \right|_{\delta=0}. \quad (15)$$

In Fig. 6b we present the results for the inverse susceptibility, $1/\chi_p$, as a function of J_2 . The extrapolation to $n \rightarrow \infty$ is performed using an extrapolation scheme with leading power $1/n$ as in Eq. (10). Clearly, in the magnetically ordered Néel phase χ_p is finite as it should be. However, close to the transition to the magnetically disordered phase at $J_2^c \approx 1.14J_1$ the susceptibility becomes very large and diverges at $J_2 \approx 1.26J_1$, which is close to J_2^c . Hence, we conclude from our CCM data that there exists a valence-bond phase between the Néel-ordered phase and the orthogonal-dimer phase.

6. The Quantum J_1 - J_2 Antiferromagnet on the Stacked Square Lattice

As already mentioned in Sec. 1 the J_1 - J_2 model on the square lattice is a canonical model to study quantum phase transitions in $d = 2$.⁹⁻²¹ However, in experimental realizations of the J_1 - J_2 model the magnetic couplings are expected to be not strictly 2d, since a nonzero interlayer coupling J_\perp is always present. For example, recently Rosner *et al.*⁴⁴ have found $J_\perp \approx 0.07J_1$ for $\text{Li}_2\text{VOSiO}_4$, a material which can be described by a square lattice J_1 - J_2 model with large J_2 .^{43,44}

Therefore, in this Section we consider the influence of an interlayer coupling on the GS phases of the the J_1 - J_2 spin-1/2 HAFM, i.e., we consider the HAFM on the stacked square lattice described by

$$H = \sum_n \left(J_1 \sum_{\langle ij \rangle} \mathbf{s}_{i,n} \cdot \mathbf{s}_{j,n} + J_2 \sum_{[ij]} \mathbf{s}_{i,n} \cdot \mathbf{s}_{j,n} \right) + J_\perp \sum_{i,n} \mathbf{s}_{i,n} \cdot \mathbf{s}_{i,n+1}, \quad (16)$$

where n labels the layers and $J_\perp \geq 0$ is the interlayer coupling. The expression in parentheses represents the J_1 - J_2 model of the layer n with intralayer NN bonds $J_1 = 1$ and NNN bonds $J_2 \geq 0$.

The classical GS's of the model are the Néel state for $J_2 < 0.5J_1$ and another particular collinear state for $J_2 > 0.5J_1$. The latter state (which we henceforth refer to as the collinear-columnar or, simply the collinear state) is a columnar $(\pi, 0)$ state characterized by a parallel spin orientation of nearest neighbors along the direction of one axis (say, the vertical or columnar direction) in each layer, and an antiparallel spin orientation of nearest neighbors along the perpendicular (say, horizontal or row) direction. It is well known⁹⁻²¹ that for $J_\perp = 0$ the quantum model has two corresponding GS phases with semi-classical magnetic LRO, one (Néel-like) for small $J_2 \lesssim 0.4J_1$ and one (collinear-columnar-like) for large $J_2 \gtrsim 0.6J_1$, which are separated by a magnetically disordered (quantum paramagnetic) GS phase.

For the treatment of the model of Eq. (16) with arbitrary J_\perp we apply the CCM and use both classical GS's (Néel and collinear-columnar) as reference states. Here we illustrate the CCM approach to this model only very briefly, and refer the interested reader to Ref. [62] for more details. In order to determine the GS phase transition points we calculate the order parameters for various values of J_\perp and determine those values $J_2 = \gamma_{\text{Néel}}(J_\perp)$ and $J_2 = \gamma_{\text{col}}(J_\perp)$ where the order parameters vanish. In Fig. 7a we present some typical curves showing the extrapolated order parameters (according to Eq. (11)) versus J_2 for some values of J_\perp . The magnetic order parameters of both magnetically long-range ordered phases vanish continuously as is typical for second-order transitions. We note, however, that there are arguments¹¹ that the transition from the collinear-columnar phase to the quantum paramagnetic phase should be of first order. The order parameters for both phases are monotonically increasing functions of J_\perp , and the transition points $\gamma_{\text{Néel}}$ and γ_{col} also move together as J_\perp increases. In Fig. 7b we present the dependence on J_\perp of these transition points. Close to the strictly 2d case (i.e., for small $J_\perp \ll J_1$) the in-

fluence of the interlayer coupling is largest. For a characteristic value of $J_{\perp}^* \approx 0.19J_1$ the two transition points γ_{Neel} and γ_{col} meet each other. Hence, we conclude that already for quite weak interlayer coupling the magnetically disordered quantum phase that is present in the strictly 2d model disappears, and a direct transition between the two semi-classically ordered magnetic phases occurs. This conclusion is also in agreement with the statement that there is no magnetically disordered phase in the 3d J_1 - J_2 model on the bcc lattice.^{72,73}

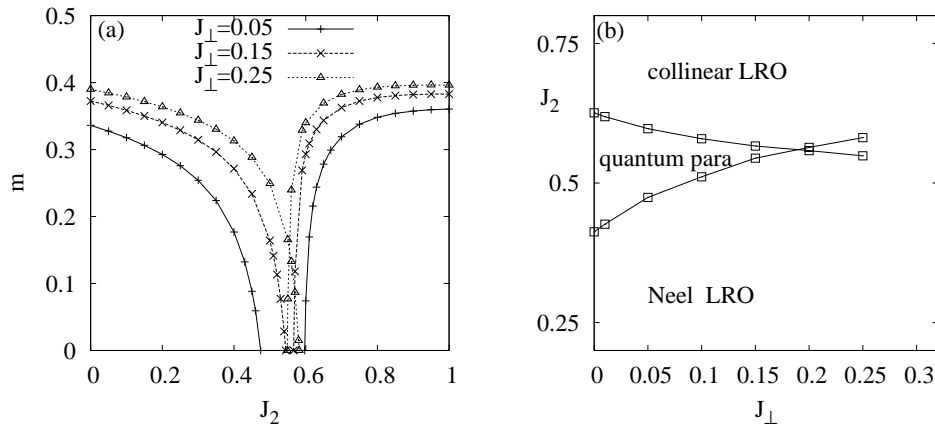


Fig. 7. (a) The magnetic order parameter m versus J_2 for various strengths of the interlayer coupling J_{\perp} (with $J_1 = 1$); and (b) the ground-state phase diagram (where the solid lines show those values of J_2 for which the order parameters vanish). Note that $J_1 = 1$.

References

1. S.T. Bramwell and M.J.P. Gingras, *Science* **294**, 14 (2001); T. Senthil, A. Vishwanath, L. Balents, S. Sachdev, and M.P.A. Fisher, *Science* **303**, 1490 (2004); G.C. Lau, R.S. Freitas, B.G. Ueland, B.D. Muegge, E.L. Duncan, P. Schiffer, and R.J. Cava, *Nature Physics* **2**, 249 (2006); R. Moessner and A.P. Ramirez, *Phys. Today* **59**, 24 (February 2006).
2. H.T. Diep (ed.), *Frustrated Spin Systems* (World Scientific, Singapore 2004).
3. U. Schollwöck, J. Richter, D.J.J. Farnell and R.F. Bishop (eds.), *Quantum Magnetism*, Lecture Notes in Physics **645** (Springer-Verlag, Berlin, 2004).
4. S. Sachdev, *Quantum Phase Transitions* (Cambridge University Press, Cambridge 1999).
5. S. Sachdev, in *Quantum Magnetism*, eds. U. Schollwöck, J. Richter, D.J.J. Farnell, and R.F. Bishop, Lecture Notes in Physics **645** (Springer-Verlag, Berlin, 2004), p. 381.
6. J. Richter, J. Schulenburg, and A. Honecker, in *Quantum Magnetism*, eds. U. Schollwöck, J. Richter, D.J.J. Farnell, and R.F. Bishop, Lecture Notes in Physics **645** (Springer-Verlag, Berlin, 2004), p. 85.
7. G. Misguich and C. Lhuillier, in *Frustrated Spin Systems*, ed. H.T. Diep, (World Scientific, Singapore, 2004), p. 229.

8. H.-J. Mikeska and A.K. Kolezhuk, in *Quantum Magnetism*, eds. U. Schollwöck, J. Richter, D.J.J. Farnell, and R.F. Bishop, Lecture Notes in Physics **645** (Springer-Verlag, Berlin, 2004), p. 1.
9. P. Chandra and B. Doucot, *Phys. Rev. B* **38**, 9335 (1988).
10. E. Dagotto and A. Moreo, *Phys. Rev. Lett.* **63**, 2148 (1989).
11. H.J. Schulz and T.A.L. Ziman, *Europhys. Lett.* **18**, 355 (1992); H.J. Schulz, T.A.L. Ziman, and D. Poilblanc, *J. Phys. I* **6**, 675 (1996).
12. J. Richter, *Phys. Rev. B* **47**, 5794 (1993); J. Richter, N.B. Ivanov, and K. Retzlaff, *Europhys. Lett.* **25**, 545 (1994).
13. L. Siurakshina, D. Ihle, and R. Hayn, *Phys. Rev. B* **64**, 104406 (2001).
14. R.F. Bishop, D.J.J. Farnell, and J.B. Parkinson, *Phys. Rev. B* **58**, 6394 (1998).
15. R.R.P. Singh, Zheng Weihong, C.J. Hamer, and J. Oitmaa, *Phys. Rev. B* **60**, 7278 (1999).
16. L. Capriotti and S. Sorella, *Phys. Rev. Lett.* **84**, 3173 (2000).
17. O.P. Sushkov, J. Oitmaa, and Zheng Weihong, *Phys. Rev. B* **63**, 104420 (2001).
18. L. Capriotti, F. Becca, A. Parola, and S. Sorella, *Phys. Rev. Lett.* **87**, 097201 (2001).
19. L. Capriotti, *Int. J. Mod. Phys. B* **15**, 1799 (2001).
20. R.R.P. Singh, Zheng Weihong, J. Oitmaa, O.P. Sushkov, and C.J. Hamer, *Phys. Rev. Lett.* **91**, 017201 (2003).
21. J. Sirker, Zheng Weihong, O.P. Sushkov, and J. Oitmaa, *Phys. Rev. B* **73**, 184420 (2006).
22. B.S. Shastry and B. Sutherland, *Physica B* **108**, 1069 (1981).
23. M. Albrecht and F. Mila, *Europhys. Lett.* **34**, 145 (1996).
24. S. Miyahara and K. Ueda, *Phys. Rev. Lett.* **82**, 3701 (1999).
25. Zheng Weihong, J. Oitmaa, and C.J. Hamer, *Phys. Rev. B* **65**, 014408 (2001).
26. A. Läuchli, S. Wessel, and M. Sgrist, *Phys. Rev. B* **66**, 014401 (2002).
27. Zheng Weihong, C.J. Hamer, and J. Oitmaa, *Phys. Rev. B* **60**, 6608 (1999).
28. E. Müller-Hartmann, R.R.P. Singh, C. Knetter, and G.S. Uhrig, *Phys. Rev. Lett.* **84**, 1808 (2000).
29. A. Koga and N. Kawakami, *Phys. Rev. Lett.* **84**, 4461 (2000).
30. C.H. Chung, J.B. Marston, and S. Sachdev, *Phys. Rev. B* **64**, 134407 (2001).
31. S. Miyahara and K. Ueda, *J. Phys.: Condens. Matter* **15**, R327 (2003).
32. M. Al Hajj, N. Guihéry, J.-P. Malrieu, and B. Bocquillon, *Eur. Phys. J. B* **41**, 11 (2004).
33. R. Darradi, J. Richter, and D.J.J. Farnell, *Phys. Rev. B* **72**, 104425 (2005).
34. B. Canals and C. Lacroix, *Phys. Rev. Lett.* **80**, 2933 (1998).
35. R. Moessner, *Can. J. Phys.* **79**, 1283 (2001).
36. D. Schmalfuß, J. Richter, and D. Ihle, *Phys. Rev. B* **70**, 184412 (2004).
37. M. Enderle, C. Mukherjee, B. Fak, R.K. Kremer, J.-M. Broto, H. Rosner, S.-L. Drechsler, J. Richter, J. Malek, A. Prokofiev, W. Assmus, S. Pujol, J.-L. Raggazoni, H. Rakato, M. Rheinstädter, and H.M. Ronnow, *Europhys. Lett.* **70**, 237 (2005).
38. T. Masuda, A. Zheludev, A. Bush, M. Markina, and A. Vasiliev, *Phys. Rev. Lett.* **92**, 177201 (2004); S.-L. Drechsler, J. Málek, J. Richter, A.S. Moskvin, A.A. Gippius, and H. Rosner, *Phys. Rev. Lett.* **94**, 039705 (2005).
39. S.-L. Drechsler, J. Richter, J. Málek, A.S. Moskvin, A. Klingeler, and H. Rosner, *J. Magn. Magn. Mater.* **290-291**, 345 (2005).
40. S.-L. Drechsler, J. Richter, A.A. Gippius, A. Vasiliev, A.S. Moskvin, J. Málek, Y. Prots, W. Schnelle, and H. Rosner, *Europhys. Lett.* **73**, 83 (2006).
41. S. Taniguchi, T. Nishikawa, Y. Yasui, Y. Kobayashi, M. Sato, T. Nishioka, M. Kontani, and K. Sano, *J. Phys. Soc. Jpn.* **64**, 2758 (1995).

42. H. Kageyama *et al.*, *Phys. Rev. Lett.* **82**, 3168 (1999).
43. R. Melzi, P. Carretta, A. Lascialfari, M. Mambrini, M. Troyer, P. Millet, and F. Mila, *Phys. Rev. Lett.* **85**, 1318 (2000).
44. H. Rosner, R.R.P. Singh, Zheng Weihong, J. Oitmaa, S.-L. Drechsler, and W.E. Pickett, *Phys. Rev. Lett.* **88**, 186405 (2002).
45. C.K. Majumdar and D.K. Gosh, *J. Math. Phys.* **10**, 1388 (1969).
46. J. Schulenburg, A. Honecker, J. Schnack, J. Richter, and H.-J. Schmidt, *Phys. Rev. Lett.* **88**, 167207 (2002); J. Richter, J. Schulenburg, A. Honecker, J. Schnack, and H.-J. Schmidt, *J. Phys.: Condens. Matter* **16**, 779 (2004).
47. F. Coester, *Nucl. Phys.* **7**, 421 (1958); F. Coester and H. Kümmel, *ibid.* **17**, 477 (1960).
48. R.F. Bishop, in *Microscopic Quantum Many-Body Theories and Their Applications*, eds. J. Navarro and A. Polls, Lecture Notes in Physics **510** (Springer-Verlag, Berlin, 1998), p. 1.
49. M. Roger and J.H. Hetherington, *Phys. Rev. B* **41**, 200 (1990).
50. R.F. Bishop, J.B. Parkinson, and Y. Xian, *Phys. Rev. B* **44**, 9425 (1991).
51. R.F. Bishop, R.G. Hale, and Y. Xian, *Phys. Rev. Lett.* **73**, 3157 (1994).
52. R. Bursill, G.A. Gehring, D.J.J. Farnell, J.B. Parkinson, T. Xiang, and C. Zeng, *J. Phys.: Condens. Matter* **7**, 8605 (1995).
53. C. Zeng, D.J.J. Farnell, and R.F. Bishop, *J. Stat. Phys.* **90**, 327 (1998).
54. S.E. Krüger, J. Richter, J. Schulenburg, D.J.J. Farnell, and R.F. Bishop, *Phys. Rev. B* **61**, 14607 (2000).
55. R.F. Bishop, D.J.J. Farnell, S.E. Krüger, J.B. Parkinson, and J. Richter, *J. Phys.: Condens. Matter* **12**, 6887 (2000).
56. S.E. Krüger and J. Richter, *Phys. Rev. B* **64**, 024433 (2001).
57. N.B. Ivanov, J. Richter, and D.J.J. Farnell, *Phys. Rev. B* **66**, 014421 (2002).
58. R. Darradi, J. Richter, and S.E. Krüger, *J. Phys.: Condens. Matter* **16**, 2681 (2004).
59. D.J.J. Farnell and R.F. Bishop, in *Quantum Magnetism*, eds. U. Schollwöck, J. Richter, D.J.J. Farnell, and R.F. Bishop, Lecture Notes in Physics **645** (Springer-Verlag, Berlin, 2004), p. 307.
60. D.J.J. Farnell, J. Schulenburg, J. Richter, and K.A. Gernoth, *Phys. Rev. B* **72**, 172408 (2005).
61. S.E. Krüger, R. Darradi, J. Richter, and D.J.J. Farnell, *Phys. Rev. B* **73**, 094404 (2006).
62. D. Schmalfuß, R. Darradi, J. Richter, J. Schulenburg, and D. Ihle, *Phys. Rev. Lett.* **97**, 157201 (2006).
63. For the numerical calculations we use the program package *CCCM* (by D.J.J. Farnell and J. Schulenburg).
64. C.J. Hamer, Zheng Weihong, and P. Arndt, *Phys. Rev. B* **46**, 6276 (1992); C. J. Hamer, Zheng Weihong and J. Oitmaa *Phys. Rev. B* **50**, 6877 (1994).
65. B.S. Shastry and B. Sutherland, *Phys. Rev. Lett.* **47**, 964 (1981).
66. H.A. Bethe, *Z. Phys.* **71**, 205 (1931).
67. M.S. Makivic and H.-Q. Ding, *Phys. Rev. B* **43**, 3562 (1991); J.-K. Kim and M. Troyer, *Phys. Rev. Lett.* **80**, 2705 (1998).
68. J. Oitmaa, C.J. Hamer, and Zheng Weihong, *Phys. Rev. B* **50**, 3877 (1994).
69. S.R. White and I. Affleck, *Phys. Rev. B* **54**, 9862 (1996).
70. A.A. Aligia, C.D. Batista, and F.H.L. Eßler, *Phys. Rev. B* **62**, 3259 (2000).
71. D.V. Dmitriev and V.Ya. Krivnov, *Phys. Rev. B* **73**, 024402 (2006).
72. R. Schmidt, J. Schulenburg, J. Richter, and D.D. Betts, *Phys. Rev. B* **66**, 224406 (2002).
73. J. Oitmaa and Zheng Weihong, *Phys. Rev. B* **69**, 064416 (2004).